



Original Article

Preclinical evidence for preventive and curative effects of resveratrol on xenograft cholangiocarcinogenesis



Suyanee Thongchot^{a,b,c,d}, Alessandra Ferraresi^b, Chiara Vidoni^b, Amreen Salwa^b, Letizia Vallino^b, Yingpinyapat Kittirat^{e,f}, Watcharin Loilome^{a,e}, Nisana Namwat^{a,e,**}, Ciro Isidoro^{b,*}

^a Department of Systems Biosciences and Computational Medicine, Faculty of Medicine, Khon Kaen University, 123 Mitrabarp Highway, Khon Kaen, 40002, Thailand

^b Laboratory of Molecular Pathology, Department of Health Sciences, Università del Piemonte Orientale "A. Avogadro", Via Solaroli 17, 28100, Novara, Italy

^c Department of Immunology, Faculty of Medicine Siriraj Hospital, Mahidol University, Bangkok, 10700, Thailand

^d Siriraj Center of Research Excellence for Cancer Immunotherapy (SICORE-CIT), Research Department, Faculty of Medicine Siriraj Hospital, Mahidol University, Bangkok, 10700, Thailand

^e Cholangiocarcinoma Research Institute, Khon Kaen University, 123 Mitrabarp Highway, Khon Kaen, 40002, Thailand

^f Department of Medical Sciences, Regional Medical Sciences Center 2 Phitsanulok, Ministry of Public Health, Phitsanulok, Thailand

ARTICLE INFO

ABSTRACT

Keywords:

Cholangiocarcinoma
Autophagy
Nutraceuticals
Cancer associated fibroblasts
tumor microenvironment

Cholangiocarcinoma (CCA), the malignant tumor of bile duct epithelial cells, is a relatively rare yet highly lethal cancer. In this work, we tested the ability of Resveratrol (RV) to prevent and cure CCA xenograft in nude mice and investigated molecular mechanisms underpinning such anticancer effect. Human CCA cells were xenografted in mice that were or not treated prior to or after transplantation with RV. Tumor growth was monitored and analyzed for the markers of cell proliferation, apoptosis, and autophagy. TCGA was interrogated for the molecules possibly targeted by RV. RV could inhibit the growth of human CCA xenograft when administered after implantation and could reduce the growth or even impair the implantation of the tumors when administered prior the transplantation. RV inhibited CCA cell proliferation, induced apoptosis with autophagy, and strongly reduced the presence of CAFs and production of IL-6. Interrogation of CCA dataset in TCGA database revealed that the expression of *IL-6 Receptor (IL-6R)* inversely correlated with that of *MAP-LC3* and *BECLIN-1*, and that low expression of *IL-6R* and of *MIK67*, two pathways downregulated by RV, associated with better survival of CCA patients. Our data demonstrate that RV elicits a strong preventive and curative anticancer effect in CCA by limiting the formation of CAFs and their release of IL-6, and this results in up-regulation of autophagy and apoptosis in the cancer cells. These findings support the clinical use of RV as a primary line of prevention in patients exposed at risk and as an adjuvant therapeutics in CCA patients.

1. Introduction

Cholangiocarcinoma (CCA), the malignant tumor of the biliary tree, is classified as intrahepatic, perihilar, and distal CCA depending on the anatomical biliary tract of origin [1]. This anatomical distinction reflects different risk factors and is clinically relevant because it directs the most appropriate treatment option and informs the predictable outcome [2–4].

Cholangiocarcinoma is relatively rare in Western countries while

being more common in Eastern countries (especially Japan, China, Thailand, and South Korea), where it is frequently diagnosed in adults chronically infected with the liver fluke larvae [1,5]. It is a fact that in the last decades, CCA incidence and mortality are increasing worldwide [1,6,7]. Current management of CCA includes surgery, chemotherapy (essentially with gemcitabine and *cis*-platin), and radiotherapy, with however poor results [1,2].

Particularly, the surgical option remains limited because most of the patients are diagnosed when the disease has already spread locally and in distant organs, and because the anatomical location of the cancer is

* Corresponding author. Università del Piemonte Orientale "A. Avogadro", Department of Health Sciences, Novara Italy.

** Corresponding author. Department of Systems Biosciences and Computational Medicine, Faculty of Medicine, Khon Kaen University, 123 Mitrabarp Highway, Khon Kaen, 40002, Thailand.

E-mail addresses: nisana@kku.ac.th (N. Namwat), ciro.isidoro@med.uniupo.it (C. Isidoro).

Abbreviations

BAX	BCL2 associated X
BCL-2	B-cell lymphoma-2
BECN1	BECLIN1
CAF	Cancer associated fibroblast
CCA	Cholangiocarcinoma
CDKN1A	Cyclin dependent kinase inhibitor 1 A
IL-6	Interleukin-6
IL-6R	Interleukin-6 receptor
MAP1LC3	Microtubule-associated proteins 1 A/1 B light chain 3
MKI67	Marker of proliferation (coding for ki-67)
SQSTM1	Sequestosome 1
SIRT1	Sirtuin 1
α -SMA	Smooth muscle actin-alpha
STAT3	Signal transducer and activator of transcription 3
TCGA	The cancer genome atlas
TEM	Transmission electron microscope
RV	Resveratrol

not easily accessible [1]. Five-year survival is very low (approx. 5 %) due to the advanced stage at diagnosis, insufficient radical surgery, poor response to chemo- and radiotherapy, and relapse of chemoresistant clones [1,4]. Novel molecular therapies have been proposed based on the genomic/transcriptomic profiling of the patients, yet the clinical trials with such targeted therapies have shown little if any survival advantage in CCA patients [1,8,9]. Thus, there is an urgent need to find alternative curative approaches based on the pathological mechanisms that drive cholangiocyte transformation. An inflamed and fibrotic tumor microenvironment is a common finding in CCA, and it has been demonstrated that such desmoplastic stroma contributes to cholestasis, and cholangiocyte transformation and proliferation that eventually develop in CCA [10,11]. In the CCA tumor microenvironment, the metabolites, mitogenic factors and inflammatory cytokines with autocrine and paracrine action secreted by tumor cells and stromal cells (mainly CAFs, cancer associated fibroblasts) mutually support the metabolic activity and proliferation of both tumor and stromal cells [12,13]. CAFs, with their secretion (particularly IL-6), have been shown to promote CCA progression, chemoresistance, invasion and metastasis, thus influencing the clinical outcome [14–18].

Recently, we succeeded in interrupting the cross-talk between CAFs and CCA cells *in vitro* [19]. By pre-treating CAFs with the nutraceutical resveratrol (RV), a strong autophagy inducer [20] with anti-cancer potential [21,22], we could limit the secretion of IL-6, and this resulted in reduced proliferation and migration of CCA cells exposed to the conditioning medium of RV-cured CAFs [19]. Interestingly, we could demonstrate that this effect was due to restoration of autophagy otherwise inhibited by IL-6 in CCA cells.

It remains to demonstrate whether this promising finding can be translated in the clinics. In view of the possible utilization of RV as an adjuvant/complementary treatment of CCA patients, we tested its preventive and curative potential in a pre-clinical animal model of xenografted human CCA cell transplant.

Here we show that the growth of human CCA xenografted in nude mice could be prevented or inhibited by pre- or co-administration of RV, and this effect was associated with reduced CAFs infiltration and expression of IL-6 and restoration of autophagy.

2. Materials and methods

2.1. In vivo experiments

Male BALB/cA Jcl-nu/nu mice aged 4 weeks and with the average

weight of 15.06 g were acclimatized 1 week before the experiments. Transplanted tumors were established by subcutaneous injection of human CCA KKU-213 cell line, at 1.5×10^6 cells/mouse at the 7th week. The mice ($n = 5$ per group) were randomly assigned to three groups as follow: (i) untreated control transplanted with tumor at week 7 (control, group a); (ii), pre-treated with RV for 2 weeks before tumor transplantation (i.e., from week 5–7) and RV-treated throughout the experimental period (preRV + RV, group b); and (iii) treated with RV one week after tumor transplantation, i.e. from week 8 (RV, group c). Note that the mice of the “control” untreated (group a) and RV-treated (group c) groups were randomly assigned to either group at week 8, i.e., one week after the xenotransplantation. In detail, the untreated control group (a) received sterile water containing the vehicle 0.1 % v/v dimethyl sulfoxide (DMSO) starting one week after tumor injection until sacrifice at week 12; mice in preRV + RV group (b) were given RV (Sigma, St. Louis, MO) dissolved in DMSO and diluted in sterile water to a concentration of 50 mg/kg, two weeks before tumor inoculation, then continued RV treatment until sacrifice at week 12; RV group (c) were given RV 50 mg/kg after one week of tumor injection and until sacrifice at week 12. Mice were allocated in individual cage and closely monitored for assuring the intake of water supplemented with RV or vehicle. The study protocol was approved with the following criteria: i) all mice were euthanized 5 weeks after tumor implant; ii) all mice were sacrificed when the tumor size of the control group was greater than 10 mm in diameter and iii) all mice were sacrificed when the size of the tumor in the experimental group was significantly different compared to the control group.

Mice body weight was recorded, and tumor diameter was determined with a vernier caliper every 3 days starting from 1 week after injection and until sacrifice at week 12. Tumor volume was calculated using the standard formula: tumor volume = (width)² x (length)/2, where the width is the smaller of the two dimensions [23]. Finally, at week 12 the mice were euthanized, the blood was withdrawn, and the tumors were dissected out, weighed, and fixed in 4 % of buffered formalin for further study. Archival hematoxylin and eosin (H&E)-stained slides for each case were reviewed by a pathologist.

2.2. Enzyme-linked immunosorbent assay

Blood samples were drawn into microtubes from an antecubital vein immediately before euthanasia. Tubes were kept and centrifuged for 15 min at 1000×g, at room temperature. Plasmas were separated from red cells and stored at –80 °C until the concentration of IL-6 was determined by commercially available IL-6 ELISA assay (R&D Systems Inc., Minneapolis, MN, USA), according to the manufacturer’s protocol. Each sample was triplicated.

2.3. Double immunofluorescent labeling

Sections of 4-μm thick, formalin-fixed, and paraffin-embedded tissues of tumor sections collected from mouse xenograft were stained with antibodies for IL-6 and α -SMA. Briefly, the tumor sections were deparaffinization, incubated in 0.3 % H₂O₂ for 30 min and then with anti-IL-6 (1:100, Abcam, Cambridge, MA, USA), anti- α -SMA (1:100, Abcam), anti-LC3 (1:100, Abcam), anti-CD68 (1:100, Abcam), and anti-panCK (1:500, Santa Cruz Biotechnology Inc., CA) at 4 °C for one night in a humid chamber. Finally, the coverslips were co-incubated with secondary antibodies, Alexa Fluor™ 488 (green, Invitrogen, Thermo Fisher Scientific, Carlsbad, CA, USA) and Alexa Fluor™ 555 (red, Invitrogen, Thermo Fisher Scientific) in the dark. Nuclei were stained with 4,6-diamidino-2-phenylindole (DAPI, Sigma-Aldrich Corp.; 1:500 dilution; 3 h at room temperature, in dark). The coverslips were sealed with fluorescence mounting medium (SlowFade™ reagent (Invitrogen, Thermo Fisher Scientific)). Confocal imaging of the coverslips was conducted on a Zeiss LSM 800 (Carl Zeiss, Jena, Germany) at Khon Kaen University and the Division of Molecular Medicine, Faculty of Medicine Siriraj Hospital, Mahidol University. Equipment details of the microscope as follow:

AxioObserver7, objective lens: Plan-Apochromat 63 \times /1.4NA oil immersion and laser: Diode 561 nm. Acquisition software was ZEN 2.3 software (blue edition, 2002–2011).

2.4. Immunohistochemical staining

Immunohistochemical staining was performed on 4- μ m sections to determine the expression of IL-6 (1:500, Abcam), α -SMA (1:1,000, Abcam), Ki-67 (1:300, Abcam), LC3 (1:1,000, Abcam), p62 (1:500, Abcam), BECLIN1 (1:100, Abcam), and p21 (1:100, Abcam). The intensity and percentage of positively stained cells were assessed under a light microscope (Carl Zeiss Axio Scope; A1 microscope) at a low-powered field (\times 100) and then evaluated at a high-powered field (\times 400).

The intensity of immunostaining was scored as weak = 1, moderate = 2, and strong = 3, also considering the percentage of positive cells as follow: 0 % = negative; 1–25 % = +1; 26–50 % = +2; and >50 % = +3.

2.5. Protein preparation and western blotting

A 75 mg of tumor tissue was homogenized with 1 mL of ice-cold RIPA lysis buffer (0.5 M NaF, 0.2 M NaVO₄, 1 M Tris-HCl pH 7.5, 0.5 M EDTA, 2.5 M NaCl, 10 % (v/v) NP-40, 10 % (w/v) SDS, Triton x-100 and deionized water) with protease and phosphatase inhibitors. Protein concentration was determined using sulforhodamine B (SRB) protein assay (Thermo Fisher Scientific, Thermo Scientific™). 30 μ g of protein lysate was electrophoresed through SDS-PAGE gels and blotted onto a polyvinylidene fluoride membrane (Bio-rad, Laboratories Ltd., UK). The membrane was blocked in 5 % non-fat dried milk diluted in 1 \times TBS/0.1 % Tween-20. Primary antibodies against interested proteins were incubated overnight followed by secondary antibodies for 1 h. The membranes were also stained for β -actin as an internal control of protein loading. Immunoreactive protein bands were visualized by Enhanced Chemiluminescence Plus solution (ECL; PerkinElmer, Waltham, MA) with the Amersham ImageQuant LAS 600 series (GE Healthcare, Life Sciences, Marlborough, MA, USA). Intensity of the bands was estimated by densitometry using Quantity One Software (BioRad, Laboratories Ltd., UK).

2.6. TUNEL staining

To evaluate apoptosis in tumors, the terminal deoxynucleotidyl transferase (TdT)-mediated deoxyuridine triphosphate (dUTP) nick end labeling (TUNEL) assay was performed using In Situ Cell death detection kit, POD (Roche Molecular Biochemicals, Germany) according to the manufacturer's protocol. Briefly, tumor sections were incubated with 20 μ g/mL proteinase K and then 0.3 % H₂O₂, labeled with fluorescein dUTP TUNEL solution in a humid and dark box for 60 min at 37 °C. TUNEL-positive stained cells were counted at \times 1000 magnification, in 5 high-power fields, by ZEISS LSM 800 Confocal Laser Scanning Microscope (Carl Zeiss Microscopy GmbH). Slides were then combined with converter-POD, stained with diaminobenzidine tetrahydrochloride (DAB) and counterstained with Mayer's Hematoxylin. TUNEL-positive cells were visualized with light microscope (Carl Zeiss Axio Scope; A1 microscope).

2.7. Transmission electron microscopy (TEM)

Tumor tissues were fixed with a solution containing 2 % glutaraldehyde plus 2 % paraformaldehyde in 0.2 M cacodylate and 0.2 M phosphate buffer, pH 7.4. After fixation, the samples were washed and treated with 0.1 % Millipore-filtered cacodylate buffered tannic acid, postfixed with 1 % buffered osmium tetroxide for 30 min, and stained and blocked with 1 % Millipore-filtered uranyl acetate. The samples were dehydrated in increasing concentrations of ethanol, infiltrated, and embedded in LX-112 medium. The samples were polymerized in a 60 °C oven for 2 days. Ultrathin sections (65 nm) were stained with 2 % uranyl

acetate and Reynold's lead citrate and imaged using a JEOL JEM-1011 TEM (JEOL USA, Inc., MA) at 100.0 KV. Images were captured using a side-mount AMT 2 k digital camera (Advanced Microscopy Techniques, Danvers, MA).

2.8. TCGA database interrogation

We have collected data on cholangiocarcinomas from cBioportal publicly available online platform (www.cbiopal.org). The dataset that we interrogated from the Cancer Genomic Atlas Project (TCGA, Firehose Legency) report a total number of 35 cholangiocarcinoma patients/samples (including intrahepatic, perihilar, and extrahepatic cancer subtypes). Patients were grouped based on the level of mRNA expression. Low versus high groups were defined relative to the median expression level of overall patient cohort and then we analyzed the cross-comparison between pair of genes based on mRNA expression groups for the following genes: *IL6R*, *BECN1*, *MAP1LC3B*, *CDKN1A*, *STAT3* and *MKI67*. To reduce the potential bias from dichotomization, the mRNA expression levels of all genes were compared based on high and low expression-based groups using *t*-test (Welch two Sample *t*-test). All cut-off values were set before the analysis, and all the tests were two-tailed.

Survival analysis was performed using SAS software for the following genes: *IL6R*, *STAT3*, and *MKI67* based on the level of mRNA expression (high vs low expression group). Survival curves of these two groups were estimated by the Kaplan–Meier plots and compared using the Cox's regression model assuming an ordered trend for the two groups. The log-rank test has been used to determine the statistical significance. The *p*-value <0.05 was considered significant. All statistical analyses were performed by using R (3.6.1 version, The R Foundation for Statistical Computing, Vienna, Austria) and SAS software (9.4 version, SAS Institute Inc., Cary, NC).

The DAVID bioinformatics functional annotation tool (<https://david.ncifcrf.gov/summary.jsp>, accessed on September 28, 2023) was used to analyze Gene Ontology (GO) biological processes, and Kyoto Encyclopedia of Genes and Genomes (KEGG) pathways were obtained with the help of positive and negative Differentially Expressed Genes (DEGs). Data are presented in bar graphs displaying the number of transcripts belonging to each positively associated biological process. Based on the different expression values, MeV4 (<http://mev.tm4.org/>, accessed on September 25, 2023), a freely available software application, was used to create heatmaps.

2.9. Statistical analysis

The values were represented as mean \pm standard deviation (SD) from three independent assays. All statistical calculations were performed with the SPSS version 19.0 (SPSS Inc., Chicago, IL). The data from two groups were analyzed by paired Student's *t*-test and from multiple groups by one-way repeated-measure analysis of variance (ANOVA) followed by Tukey's post-hoc test using GraphPad Prism software version 5.01 (GraphPad Software, Inc.) or SigmaPlot 16.0v (Systat Software, Inc.). *P* < 0.05 was considered to indicate a statistically significant difference.

3. Results

3.1. RV elicits preventive and curative effects on cholangiocarcinoma xenografts in nude mice

We used a subcutaneous xenograft model of human CCA in male nu/nu mice to determine the preventive and therapeutic potential of orally administered RV. For this purpose, we set two protocols: (i) in the “preventive” protocol (preRV + RV), RV treatment started two weeks prior the xenotransplantation and continued throughout the whole experimental period, while (ii) in the “curative” protocol the treatment

with RV started one week after the xenotransplantation. A third group was treated with the vehicle and served as “control”. The treatment timeline is schematized in Fig. 1A. Representative images of the subcutaneous growth of the tumor in the three groups are shown in Fig. 1B.

To monitor the growth, the volume of the subcutaneous tumor mass was roughly measured throughout the experimental period with a caliper (Fig. 1C). At the end of the experiment, the mice were euthanized, and the tumors excised, photographed (Fig. 1D) and weighted (Fig. 1E), and the volume was measured (Fig. 1F). Taken together, the results showed that (i) all mice ($n = 5$) in the control (untreated) group developed the tumor; (ii) in the preRV + RV “preventive” group ($n = 5$) two mice (numbered 4 and 5) did not develop at all a detectable tumor mass and three mice developed a tumor of very small volume (approx. 1/25 that of the controls); (iii) in the RV “curative” group all the mice ($n = 5$) developed a tumor of small volume (approx. 1/5 that of controls). Quantitatively, in five weeks (from 7 to 12) the five tumors in the control group reached a volume of approximately 5.00 mm^3 and an average weight of 2.1 g, while in the preventive group the three tumors showed an average volume of 0.15 mm^3 and weight of 0.1 g, and in the curative group the five tumors showed an average volume of 1.0 mm^3 and weight of 0.2 g. When differences in the tumor volume (mm^3) were expressed as percentages, the preventive and curative RV protocols elicited a 95 % and a 75 % inhibition of the tumor growth, respectively (Fig. 1G). Worthy of note, potential toxicity of the treatments could be excluded based on animal behavior in terms of food and drink intake and gain of weight (Fig. 1H).

3.2. RV greatly reduces the presence of cancer associated fibroblasts and the production of inflammatory IL-6 in the stroma of CCA xenografts

The tumor microenvironment of CCA is characterized by a desmoplastic stroma rich of CAFs producing inflammatory cytokines, among which IL-6 is predominant [16,18]. Previously, we have shown that *in vitro* RV can cure CAFs and limit their production of IL-6 [19]. We asked whether such an effect could be reproduced *in vivo* as well. Further, we considered also the possible contribution by macrophages in the secretion of IL-6 in the stroma. We performed the immunostaining of IL-6 and of α -SMA (a marker of CAFs), and of IL-6 and of CD68 (a marker of macrophages) in three sections of each CCA tumor. RV treatment significantly reduced the expression of IL-6 and α -SMA (Fig. 2A) but only slightly reduced CD68 positivity, indicating that RV prominently reduced CAFs infiltration while eliciting a minor effect on macrophages in the stroma (Fig. 2C). This suggests that IL-6 was primarily produced by CAFs. Furthermore, cytokeratin or PanCK staining (a marker of cancer cells) confirmed that RV treatment reduced CAFs but not invasive tumor cells (Fig. 2B). Representative images and the relative semi-quantitative analysis of the staining (Fig. 2D and E) demonstrate that RV significantly reduced the presence of CAFs and IL-6 in the tumor. This was confirmed by western blotting of the whole homogenates, which showed decreased expression of IL-6 and of α -SMA in the tumors of the preventive and curative RV groups compared to the controls (Fig. 2F and G). Finally, we assayed the plasma level of circulating IL-6 in CCA-bearing mice at the end of the treatments and found that it was nearly halved in those pretreated or treated with RV (Fig. 2H). It is to be noted that in the preRV + RV group, the mice not developing detectable tumor mass ($n = 4$ and 5) had the lowest level of circulating IL-6.

3.3. RV blocks cell proliferation and induces apoptosis in CCA xenograft

In search for the mechanisms underlying the preventive and curative effects of RV, we first analyzed the tumors for markers of cell proliferation and cell death. The nuclear staining of Ki-67, which reflects the rate of cell proliferation, was greatly reduced whereas the staining for p21, which parallels a cell cycle block, was greatly increased in tumors from preventive and curative mice groups treated with RV (Fig. 3A). The latter also showed increased TUNEL staining, which is indicative of

apoptosis (Fig. 3B). In confirmation of induced apoptosis, in the tumors from preventive and curative RV groups of mice the expression of the pro-apoptotic protein BAX was increased while that of the anti-apoptotic protein BCL-2 was decreased (Fig. 3C). The BAX/BCL-2 ratio was 4-fold and 3-fold greater than controls in the preventive and curative groups of tumors, respectively ($p < 0.001$ and $p < 0.05$, respectively) (Fig. 3D).

3.4. RV induces autophagy in cholangiocarcinoma xenograft

Previous data consistently demonstrate that RV can prevent and cure CCA in nude mice via inducing a cell proliferation block and apoptosis. RV has been shown to also induce autophagy as a mechanism for blocking the growth of cancer cells, both *in vitro* and *in vivo* models of various types of cancers [24–27]. We therefore investigated whether autophagy was involved in the preventive and curative effects of RV. Electron microscopy imaging demonstrated an increased accumulation of autophagic vacuoles in the tumors from the preventive and curative RV-treated groups (Fig. 4A). Next, we performed the immunostaining of three autophagy markers, namely LC3, a marker of autophagosomes and autolysosomes, p62/SQSTM1, a marker of the autophagy cargo being degraded, and BECLIN-1, a signaling protein triggering the formation of autophagosomes [28]. LC3 and BECLIN-1 staining increased while that of p62/SQSTM1 decreased in the tumors from the preventive and curative RV-treated mice, consistent with induction of autophagy (Fig. 4B). To further confirm these findings, we assayed the expression of these proteins by western blotting. The conversion of LC3-I into LC3-II isoform roughly reflects the rate of autophagosome formation, while the decrease of p62 indirectly mirrors the rate of autophagy degradation [28]. Overall, the tumors from the preventive and curative RV-treated mice confirmed the up-regulation of autophagy, as indicated by the increased level of LC3-II (*vs* LC3-I), the decreased level of p62/SQSTM1, and the increased expression of BECLIN-1 (Fig. 4C).

3.5. Translational significance of the molecular pathways targeted by RV treatment in human cholangiocarcinoma

We have interrogated the TCGA database to search for the clinical relevance of the molecules targeted by RV in human CCA. The oncoprint reporting the gene alterations (including copy number variation, deletion, mutations) and the mRNA expression of the relevant genes (i.e., *MKI67*, *IL-6R*, *STAT3*, *BECN1*, and *MAP1LC3B*) is shown in Supplementary Fig. S1. TCGA data are available for only 35 CCA patients, which makes difficult to reach the statistical significance, and therefore the analysis shows a trend rather than a significant correlation between the expression of these genes and with the clinical outcome. Additionally, only 5 tumors express high level of *MAP1LC3B* mRNA. Nonetheless, the trend is that: (i) the expression of *IL-6R* inversely correlates with that of *MAP1LC3B* and of *BECN1* genes; (ii) the tumors with low expression of *CDKN1A* (coding for p21) also express low level of *MAP1LC3B* (Fig. 5A); (iv) the expression of *IL-6R* positively correlated with that of *STAT3* (Supplementary Fig. 2A); (v) the tumors with low expression of *BECN1* express high level of *STAT3* (Supplementary Fig. S2B). More importantly, the data also indicate that the low expression of *IL-6R* and of its downstream effector *STAT3* as well as that of *MKI67* (coding for ki-67) associates with better survival (Fig. 5B).

3.6. Differentially expressed genes in two groups of patients stratified based on *IL-6R* and *BECN1* expression

To assess the biological processes involved in the *IL-6R* differential clinical outcomes described above (Fig. 5B, upper panel), we performed an in-silico transcriptomic analysis on the CCA patient’s dataset.

We retrieved RNA-seq data (mRNA expression profile) from the TCGA database and performed a co-expression analysis to identify the most significant differentially expressed genes (DEGs) correlated with *IL-6R* expression. It was found that *IL-6R* positively correlated genes

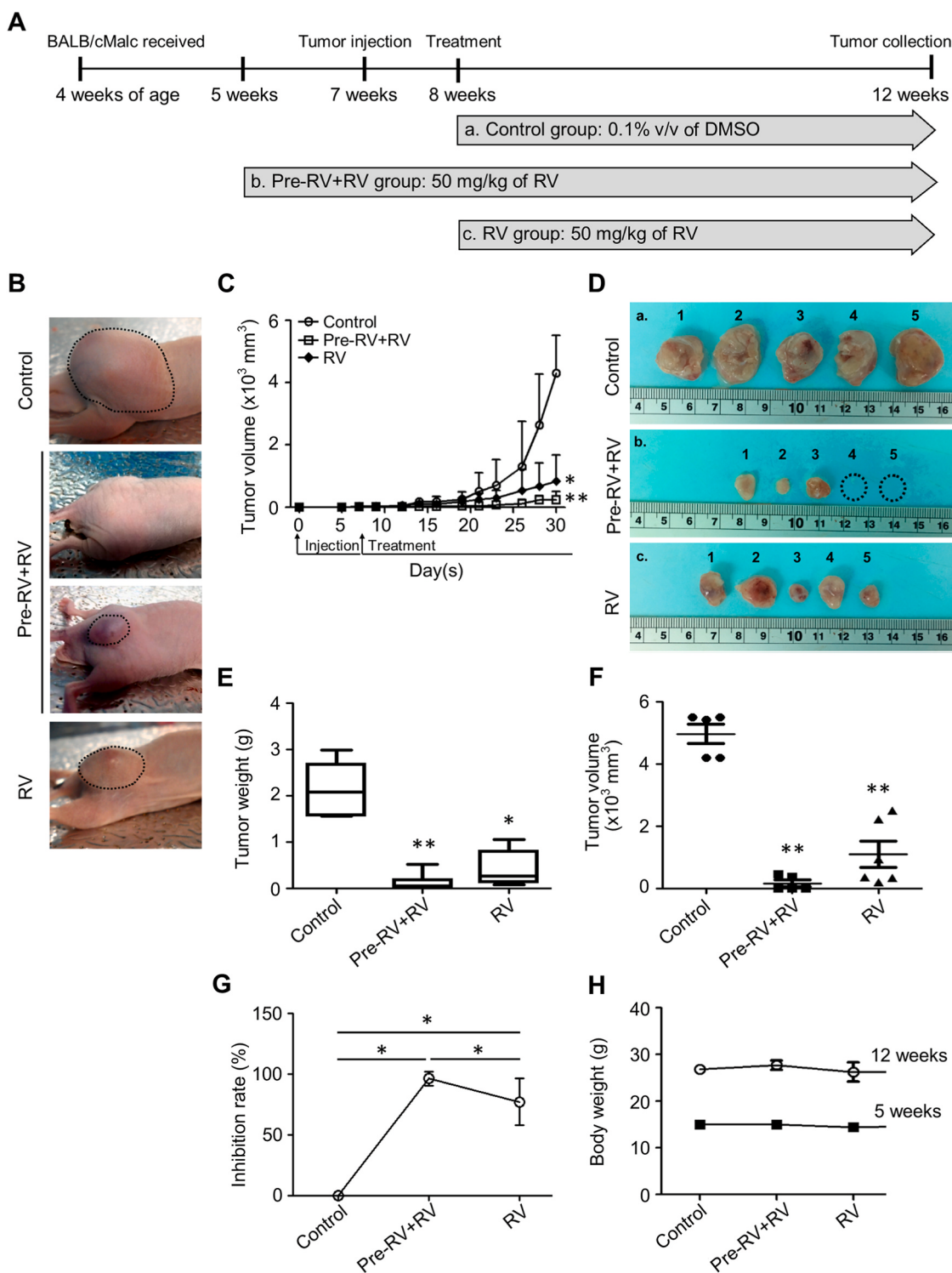


Fig. 1. RV halted the growth of KKU-213 xenograft tumor.

(A) The treatment protocol used with PreRV + RV (50 mg/kg), RV (50 mg/kg), and control (sterile water contained 0.1 % DMSO) were given in drinking water. The mice were humanely sacrificed and analyzed after RV administration for 23 days. * $p < 0.05$, ** $p < 0.01$, compared with control.

(B) Gross appearance and (C) measurement of the subcutaneous tumor growth during the experimental period.

(D) Images of the tumors from each group excised on the last day of the experimental period.

(E) tumor volume comparison measured using Vernier calipers and calculated by formula: $V = \text{length (mm)} \times \text{width (mm)} \times 0.5 \text{ width (mm)}$. * $p < 0.05$, ** $p < 0.01$, compared with control.

(F) Wet weight of tumor at 23 days of injection. ** $p < 0.01$ compared with control.

(G) Inhibition rate by PreRV + RV, and RV were presented by percentages compared to control group. * $p < 0.05$ compared with control.

(H) The change in body weight (gram) were measured three days per week during the treatment period.

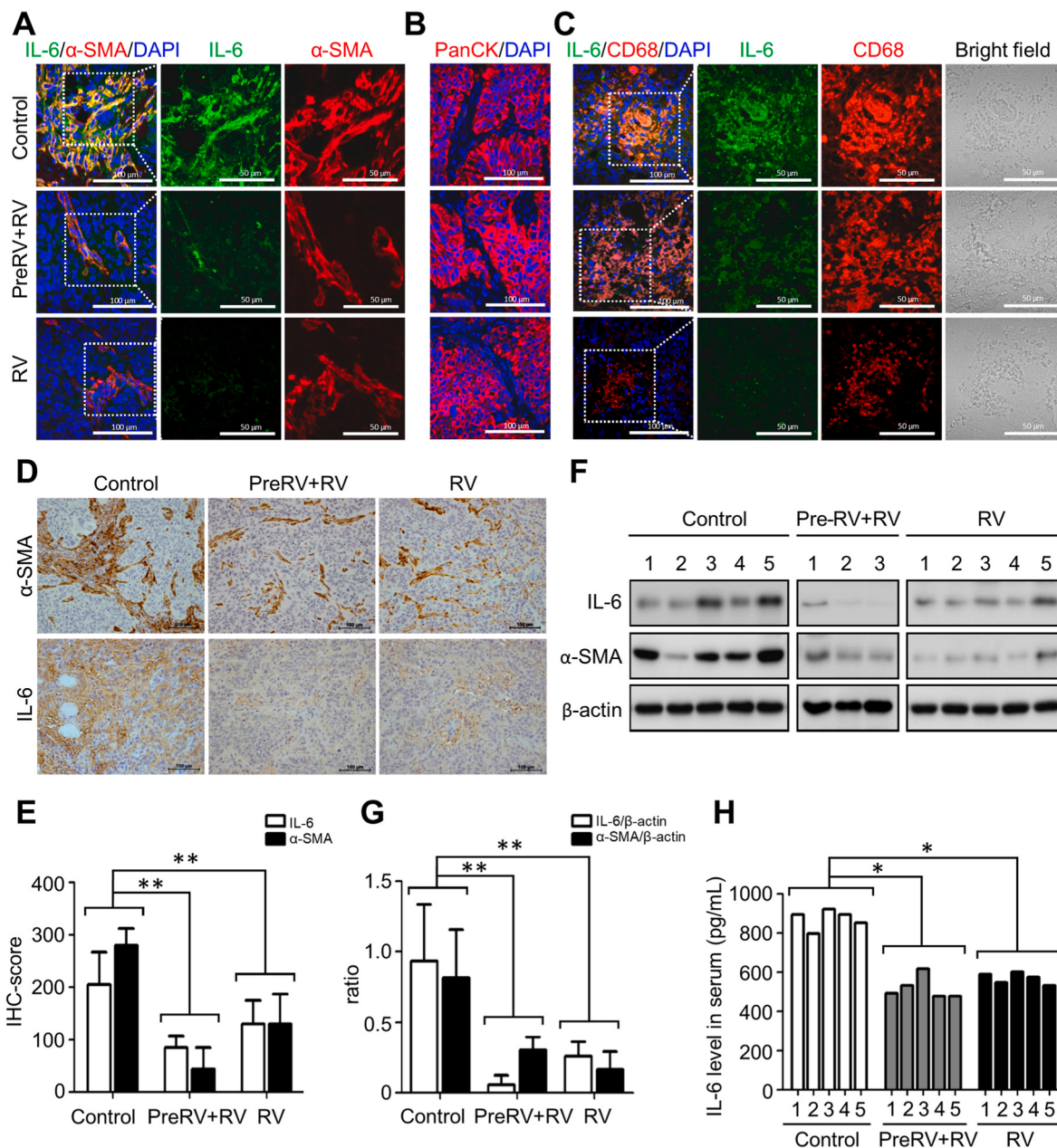


Fig. 2. RV treatment reduced the incidence of CAFs infiltration in mice. Decreased expression of IL-6 and α -SMA levels was recorded in PreRV + RV and RV-treated group.

(A) IL-6 and α -SMA expression was determined by immunofluorescence (scale bar = 100 μ m and 50 μ m; original magnification = 63 \times).

(B) The expression of panCK and of (C) CD68 was assessed by immunofluorescence staining.

(D) Immunohistochemistry (scale bar = 100 μ m; original magnification = 20 \times), and (F) western blotting of tumor tissues.

(E) IHC score and (G) densitometric data of western blotting (normalized on the loading control β -actin) are reported. **p < 0.01 compared with control.

(H) The serum IL-6 concentration was significantly decreased in PreRV + RV and RV treatment compared with control group. **p < 0.01 compared with control.

were involved in the cellular macromolecule biosynthetic process, Interleukin signaling pathway, cell migration and cell cycle (Supplementary Fig. S2).

Next, we chose the top significant genes associated with each of these biological processes and checked for their differential expression in tumors expressing high IL-6R and low BECN1 and in tumors expressing low IL-6R and high BECN1. We selected four patients for each group as follow: (i) Group A included patients with high IL-6R expression and low BECN1 expression, and (ii) Group B included patients with low IL-6R expression and high BECN1 expression. The most significant DEGs were screened and selected for each biological process and pathway from the ones identified with the help of software called David - Gene Ontology.

From the heatmaps reported in Fig. 6, one can appreciate that tumors from patients of Group B with high BECN1 and low IL-6R (showing an upregulated autophagy) display the downregulation of a range of transcripts involved in oncogenic pathways, including the Interleukin signaling, the PI3K-AKT, Wnt-cadherin and Hedgehog signaling pathways and the cell cycle. An opposite trend was observed in Group A patients, with tumors expressing high IL-6R and low BECN1, displaying the upregulation of oncogenic pathways along with the downregulation of genes involved in the regulation of autophagy, which correlates with poor prognosis. Worthy to note, the tumors expressing high BECN1 and low IL-6R showed high levels of DIRAS-3, BAX and CDKN1A mRNA and low levels of STAT3, IL6ST (IL-6 signal transducer, aka IL-6R beta),

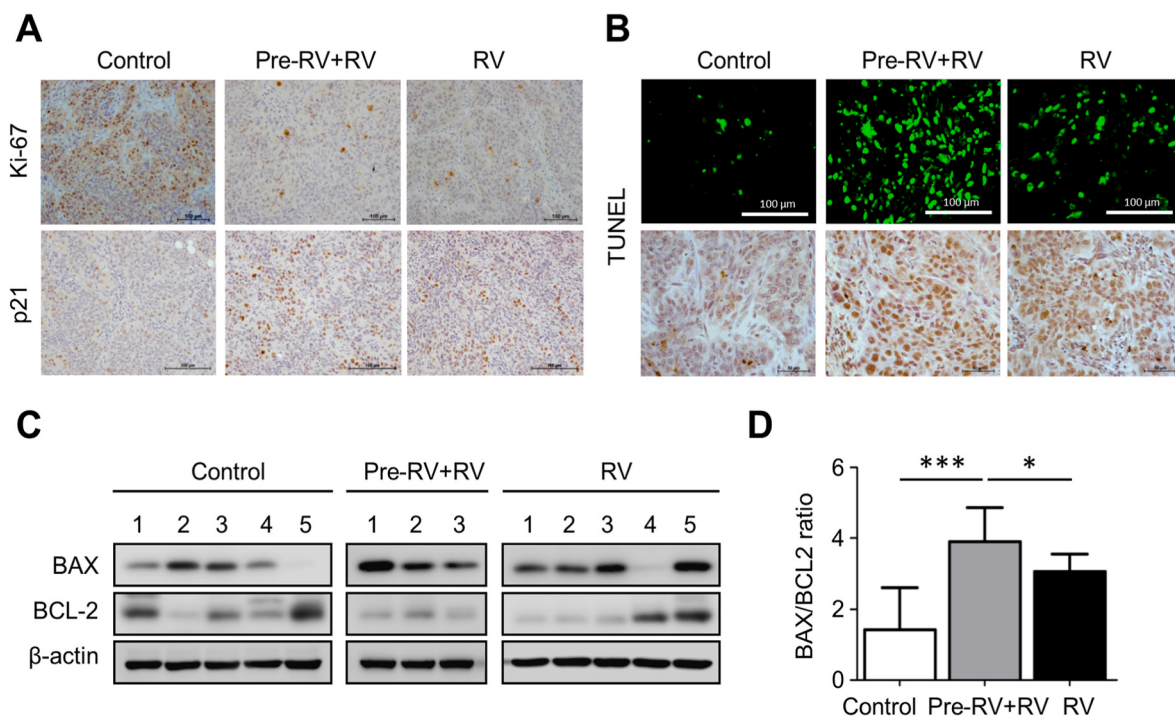


Fig. 3. RV significantly increased apoptosis cell death in PreRV + RV and RV-treated mice.

(A) Tumor slices were processed for immunohistochemical staining of Ki-67 and p21 (scale bar = 100 µm; original magnification = 20×) and for (B) *in situ* cell death TUNEL staining (POD detection kit, scale bar = 100 µm; original magnification = 63×).

(C) The expression of relevant proteins involved in apoptosis (BAX and BCL-2) was determined by western blotting assay.

(D) The induction of apoptosis was monitored by BAX/BCL-2 ratio. Densitometry of western blotting data (normalized on the loading control β-actin) are reported as mean ± SD. The ratios between BAX/BCL-2 were significantly different in PreRV + RV and RV treatment compared with control group. ***p < 0.001 and *p < 0.05 compared with control.

EGFR, MKI67, GSK3, and GLI1 mRNA.

4. Discussion

Cholangiocarcinoma is a prototype of inflammatory cancer characterized by a dysplastic stroma rich of CAFs and inflammatory cytokines [18]. CCA is an aggressive tumor, and the current therapies have a low rate of success [1,2]. Particularly, the abundance of CAFs and of their secreted IL-6 is responsible for the dismal prognosis [14,16–18]. Thus, novel therapeutic strategies are needed to prevent and cure this tumor. In a cohort of CCA patients we found that high CAFs infiltration and expression of stromal IL-6 correlated with reduced overall survival, and this was associated with inhibition of autophagy and of autophagy-dependent responsiveness to cytotoxic drugs in CCA cells [16].

Autophagy is a lysosome-mediated degradation pathway that plays a dual role in cancer progression, either promoting or inhibiting, depending on the signals present in the tumor microenvironment [29]. In fact, autophagy in cancer cells is biochemically and epigenetically regulated by tumor microenvironmental factors, including nutrients, oxygen, growth factors, and inflammatory cytokines [29–33]. Similarly, this happens also in CAFs [34]. This makes autophagy an appealing target for novel therapeutic approaches.

Previously, we have shown that CAFs-derived IL-6 stimulates the malignant behavior of CCA cells through inhibition of autophagy, and that RV could cure *in vitro* CCA-derived CAFs preventing the secretion of IL-6 and thus rescuing autophagy in CCA cells [19].

The present study aimed to test the effectiveness of RV in CCA cholangiocarcinogenesis in a pre-clinical *in vivo* setting, and to investigate the molecular mechanisms involved in its action with a focus on the microenvironment and autophagy regulation. Here, we report that the pre-treatment and treatment with RV can prevent and cure human CCA

in a nude mice xenograft model and that this effect is associated with induction of autophagy and apoptosis in cancer cells and concomitant inhibition of CAFs maturation and secretion of IL-6.

Our findings are in line with similar studies supporting the anti-cancer properties of RV. RV was shown to inhibit the growth of human breast cancer cells xenografted in nude mice by inducing apoptosis and limiting angiogenesis in the tumor [35]. In this same line, RV was shown to inhibit the growth of orthotopic xenografted colorectal cancer [36].

These authors did not investigate whether autophagy was involved in such anticancer effect, yet it was previously shown that RV causes cell growth arrest and death of colon carcinoma cells through hyper-induction of autophagy [25]. Tan et al. showed that RV injected intraperitoneally at a dose of 160 mg/kg could effectively reduce the growth of human ovarian cancer xenograft in female nude mice, and this effect was attributed to the inhibition of glucose uptake and glycolysis (i.e., by limiting the source of energy for tumor growth) and the induction of autophagy [27]. Interestingly, we have shown that in ovarian cancer RV is a strong inducer of autophagy acting as a protein and glucose-restriction mimetic [20,37]. More interestingly, RV was found to inhibit the growth of lung cancer cells transplanted in mice by inducing apoptosis and autophagy in cancer cells and by contrasting the CAF maturation [26]. Pterostilbene, an analogue of RV, was found to slow down the growth of CCA xenografted in nude mice, yet these authors did not investigate the induction of autophagy and/or apoptosis and CAF infiltration in the tumor [38]. Thus, the present study is the first one showing the ability of RV to prevent and to cure CCA in a preclinical animal model and proving that this effect is mechanistically linked with the induction of apoptosis and autophagy in cancer cells, along with inhibiting the infiltration and maturation of CAFs and reducing the release of IL-6 in the tumor microenvironment and systemically. In our model, (CD68-positive) macrophages were also shown to infiltrate the xenotransplant stroma, however RV elicited an only a slight effect on

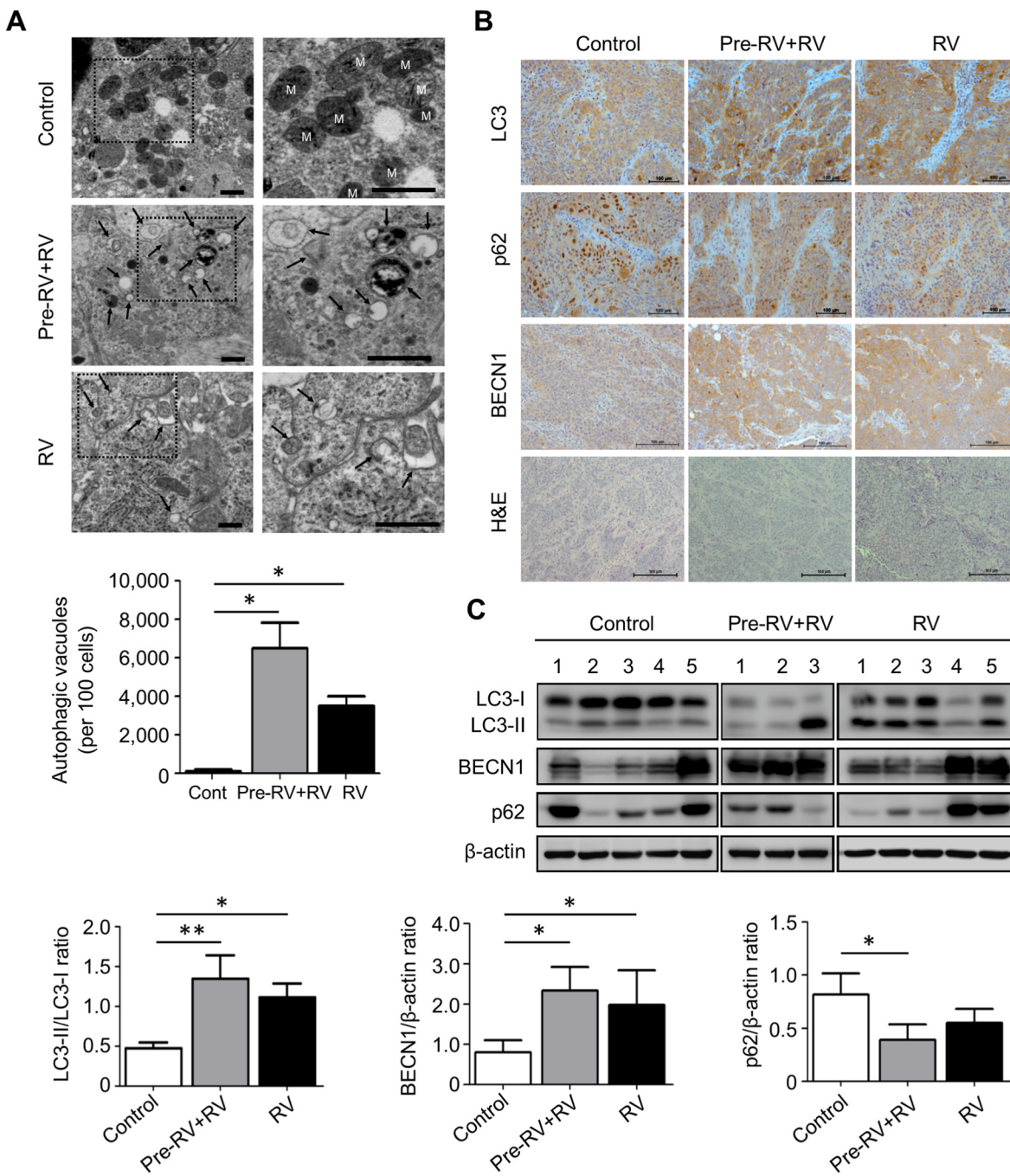


Fig. 4. Up-regulation of autophagy in Pre-RV + RV and RV-treated mice.

(A) Tumor sections were prepared for transmission electron microscope (TEM), scale bar = 1 μ m and 800 nm (original magnification = 10,000 \times). Mitochondrial damage and activation of autophagy/apoptosis in xenograft tumors derived from control, PreRV + RV, and RV were represented by TEM image and graph of quantitative analysis. *p < 0.05 compared with control.

(B) Immunohistochemistry staining for autophagic proteins (LC3, p62, and BECLIN1), and Hematoxylin-Eosin (H&E) staining (scale bar = 100 μ m; original magnification = 20 \times).

(C) Tumor tissue sections from mice were homogenized and processed for western blotting analysis to detect the expression of LC3, BECLIN1, and p62. The filter was stripped and re-probed for β -actin to verify protein loading. **p < 0.01 and *p < 0.05 compared with control.

this infiltration suggesting CAFs as the major source of IL-6. How mechanistically RV could inhibit the secretion of IL-6 by CAFs goes beyond the aim of the present work that focuses on the preventive and curative effects of RV on CCA preclinical model. What here is relevant is the ability of RV to interfere with the secretome of CAFs in the tumor microenvironment which then impacts on tumor growth. Highlighting the role of the cross-talk in the tumor microenvironment and consistent with the present findings, RV was shown to alter CAFs secretion in a way

that limited the migration, invasion and stem-like properties in breast cancer cells, an effect associated with reduced activation of the Akt and STAT3 pathways [39].

It is to be noted that the pattern of CAFs infiltrate and IL-6 along with that of autophagy markers here found in the CCA xenograft resembles that described in CCA patients' derived biopsy [16].

To further strengthen the translational value of these findings, we looked for the clinical relevance of the genes targeted by RV in the

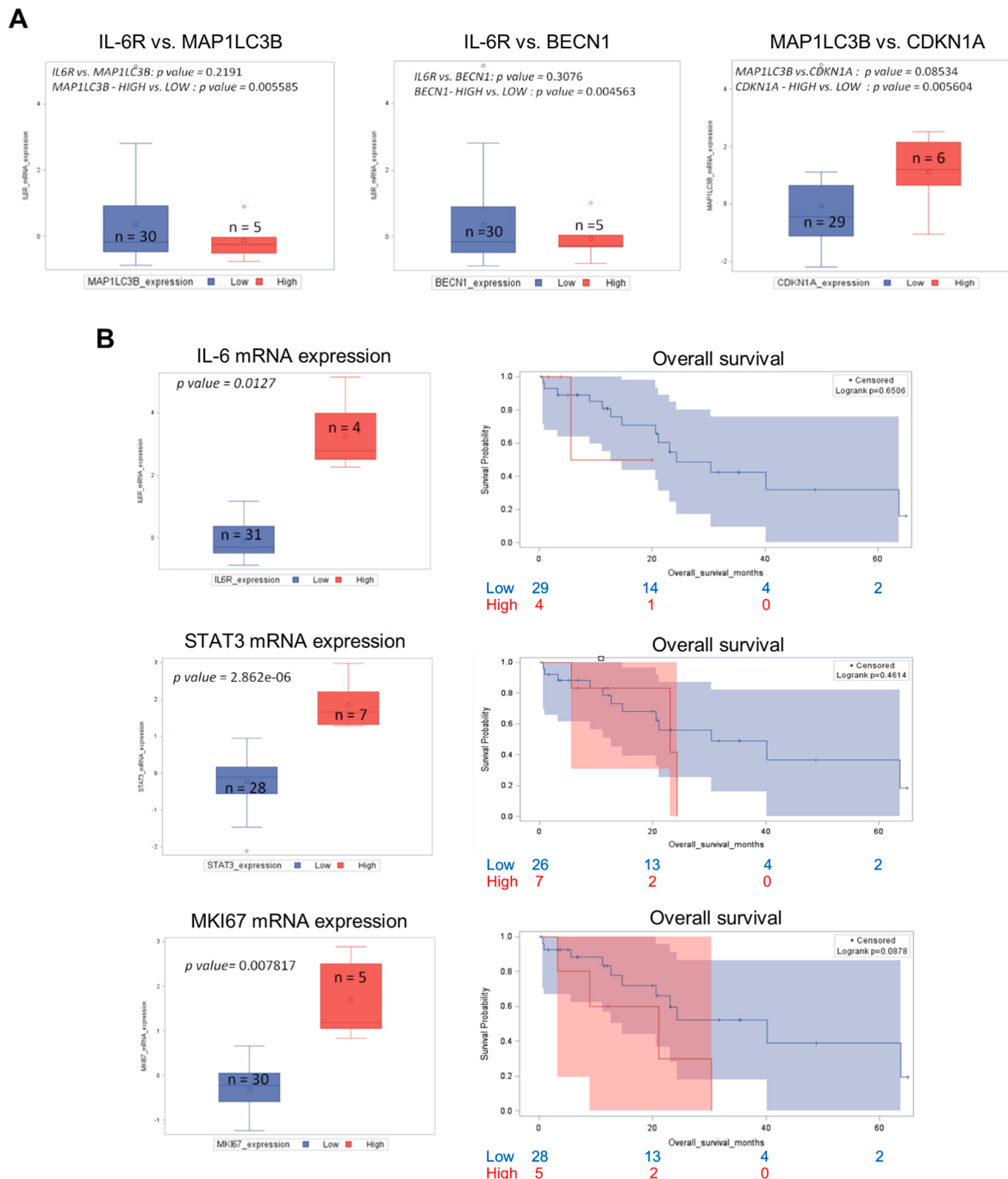


Fig. 5. Patients with downregulation of IL-6R/STAT3 pathway along with high BECLIN-1-dependent autophagy display a longer overall survival. (A) Correlation of *IL-6R* vs. *MAP1LC3B*, *IL-6R* vs. *BECN1*, and *MAP1LC3B* vs. *CDKN1A* mRNA expression in 35 cholangiocarcinoma patients. (B) The mRNA expression and the prognostic value of *IL-6R*, *STAT3*, and *MKI67* in a cohort of cholangiocarcinoma patients (TCGA, Firehose legacy).

cohort of CCA patients included in the TCGA database. Because of the small number of patients (only 35), the analysis could not reach the statistical significance. Although not statistically significant, it is clearly apparent that patients bearing a CCA with low expression of *IL-6R*, of *STAT3* (a downstream effector of IL-6 signaling) and of *MKI67* tend to survive longer. Additionally, the data suggest that any pharmacologic treatment that could interfere with the IL-6 pathway (down-regulating *IL6-R* and *STAT3*) and lower the expression of Ki67 would be beneficial for CCA patients. It is worth noting that in our experimental model, RV was able to lower the expression of IL-6 and of STAT3 (its downstream effector), of BCL-2 and of Ki-67 (the product of *MKI67*; marker of cell proliferation) while it increased the expression of p21 (the product of

CDKN1A; indicative of cell cycle arrest) and of the ATG proteins LC3 and BECLIN-1. It seems that autophagy is dysregulated in the early stage of cholangiocarcinogenesis [40]. Worthy of note, low expression of BECLIN-1 (indicative of defective autophagy) correlates with metastasis and poor prognosis in CCA [41], while high expression of LC3 (indicative of upregulated autophagy) associates with favorable prognosis in post-chirurgical CCA patients [42], and both high BECLIN-1 and low Ki-67 expression are good prognostic markers in CCA [43].

In conclusion, in this study we demonstrate that RV could inhibit the growth of human CCA xenograft when administered after implantation and could even reduce the implantation and growth of the tumors when administered prior the transplantation. This effect can be attributed to

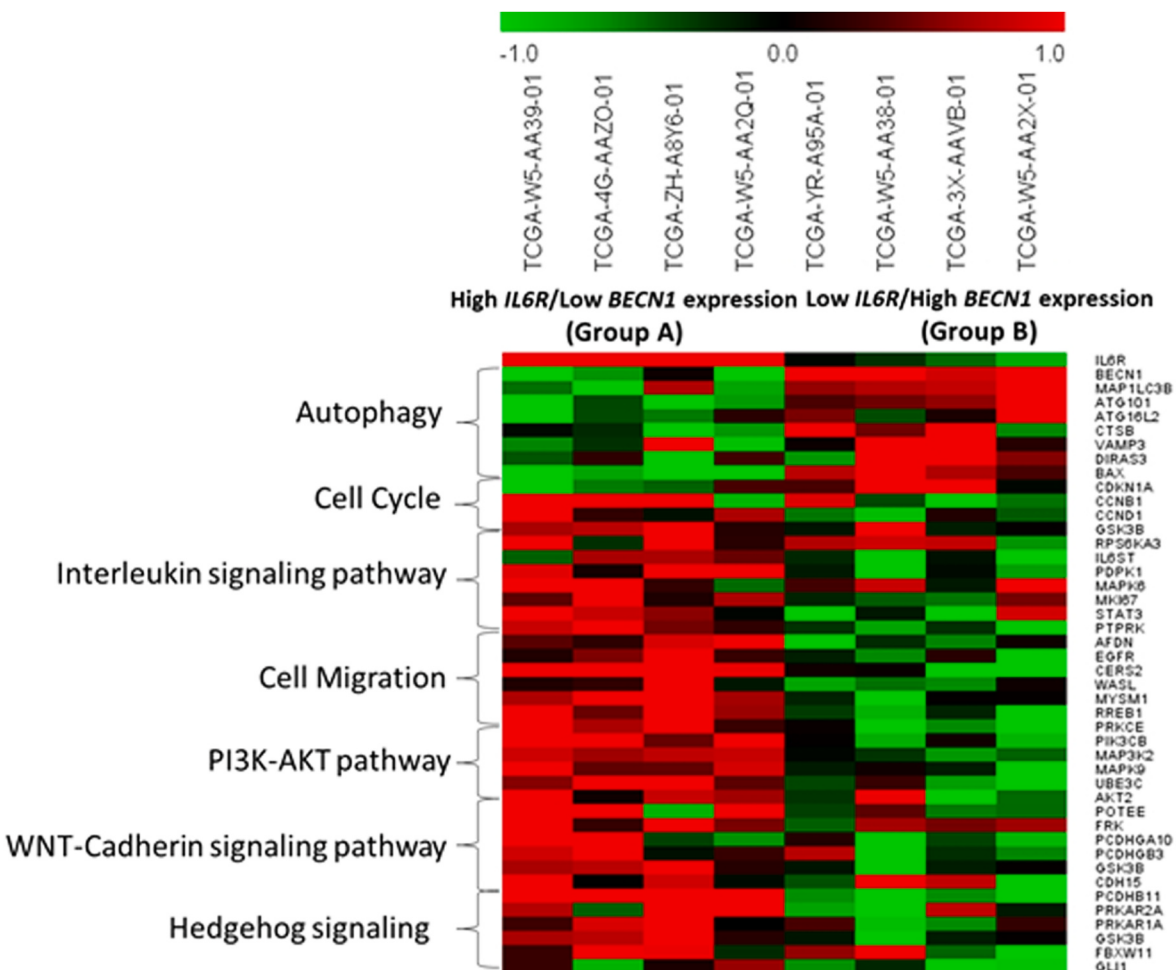


Fig. 6. Differentially expressed genes in two groups of patients stratified based on *IL6R* and *BECN1* expression.

Patients were stratified based on high *IL-6R* expression and low *BECN1* expression (Group A) and low *IL6R* expression and high *BECN1* expression (Group B).

the reduced maturation of CAFs and secretion of IL-6 and concomitant induction of autophagy and apoptosis in cancer cells.

We have recently shown that RV contrasts the IL-6 induced inhibition of autophagy and rather promotes an autophagy-dependent arrest of cancer cell growth with the feature of cell dormancy [44]. We cannot exclude that this process also contributes to the RV anti-tumor effect in our CCA xenograft model. Consistent with this hypothesis is the finding that tumors with high expression of *BECN1* and low expression of *IL6-R* showed high expression of autophagy genes, among which *DIRAS3* (aka *ARH-1*, Aplasia Ras Homolog-1), and of cell cycle arrest (*CDKN1A*), a pattern of gene expression associated with cancer cell dormancy [44]. The milieu in the tumor microenvironment can drive tumor dormancy through epigenetic regulation of autophagy [reviewed in 45], and in this context RV may play a role [33,44].

It is to be stressed that, while many studies have focused on the direct effects of RV on cancer cell proliferation, this study for the first time shows that RV can elicit antineoplastic effects by interrupting the protumorigenic metabolic and cytokine-mediated cross-talk between CAFs and cancer cells *in vivo*.

Finally, it is worth noting that RV is being considered for cancer treatment in a personalized medical approach [46,47]. The cartoon in Fig. 7 summarizes the final message with the findings here reported.

Ethics approval

All the animals were maintained according to standard guidelines of American Association for the Accreditation of Laboratory Animal Care.

The experiments were performed in full accomplishment with the internationally accepted principles for laboratory use and care and approved by the Institutional Animal Care and Use Committee (IACUC-KKU-68/60) of Khon Kaen University, Khon Kaen, Thailand.

Data availability statement

All data and materials are published in the manuscript; supplementary materials are published on the journal website or available on request.

CRediT authorship contribution statement

Suyanee Thongchot: Writing – original draft, Validation, Methodology, Investigation, Formal analysis, Data curation, Conceptualization. **Alessandra Ferraresi:** Software, Investigation, Data curation. **Chiara Vidoni:** Software, Investigation. **Amreen Salwa:** Software, Investigation. **Letizia Vallino:** Software, Investigation. **Yingpinyapat Kittirat:** Software, Investigation. **Watcharin Loilome:** Conceptualization. **Nisana Namwat:** Writing – review & editing, Supervision, Project administration, Conceptualization. **Ciro Isidoro:** Writing – review & editing, Writing – original draft, Supervision, Project administration, Conceptualization.

Declaration of competing interest

The authors declare that they have no known competing financial

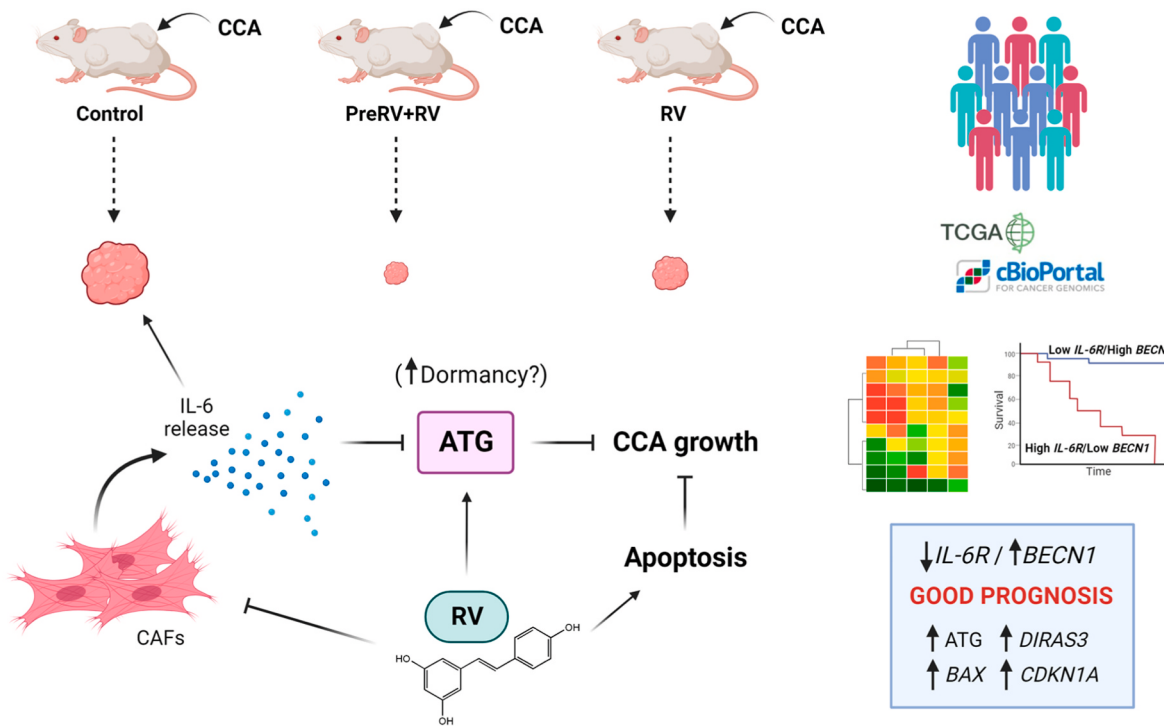


Fig. 7. Illustration of the main findings reported in the article.

interests or personal relationships that could have appeared to influence the work reported in this paper.

Acknowledgements

AF was supported by a post-doctoral fellowship granted from the Fondazione Umberto Veronesi, Milan, Italy. LV was supported by a post-doctoral fellowship granted by Department of Health Sciences, Università del Piemonte Orientale. AS is a PhD student and recipient of a fellowship granted by the Italian Ministry of University and Research (MIUR, Rome, Italy). NN was supported by NSRF under the Basic Research Fund of Khon Kaen University, Khon Kaen University, Thailand. Special thanks to Professor Chanitra Thuwajit (Department of Immunology, Faculty of Medicine Siriraj Hospital, Mahidol University, Bangkok, Thailand) for kind offer of anti-panCK antibody.

Appendix A. Supplementary data

Supplementary data to this article can be found online at <https://doi.org/10.1016/j.canlet.2023.216589>.

References

- [1] J.M. Banales, J.J.G. Marin, A. Lamarca, P.M. Rodrigues, S.A. Khan, L.R. Roberts, V. Cardinale, G. Carpino, J.B. Andersen, C. Braconi, D.F. Calvisi, M.J. Perugorria, L. Fabris, L. Boulter, R.I.R. Macias, E. Gaudio, D. Alvaro, S.A. Gradiolone, M. Strazzabosco, M. Marzoni, C. Coulouarn, L. Fouassier, C. Raggi, P. Invernizzi, J. C. Mertens, A. Monsek, S. Rizvi, J. Heimbach, B.G. Koerkamp, J. Bruix, A. Forner, J. Bridgewater, J.W. Valle, G.J. Gores, Cholangiocarcinoma 2020: the next horizon in mechanisms and management, Nat. Rev. Gastroenterol. Hepatol. 17 (9) (2020 Sep) 557–588, <https://doi.org/10.1038/s41575-020-0310-z>. Epub 2020 Jun 30. PMID: 32606456; PMCID: PMC7447603.
- [2] L.J. Palmieri, J. Lavolé, S. Dermine, C. Brezault, M. Dhooge, A. Barré, S. Chaussade, R. Coriat, The choice for the optimal therapy in advanced biliary tract cancers: chemotherapy, targeted therapies or immunotherapy, Pharmacol. Ther. 210 (2020 Jun), 107517, <https://doi.org/10.1016/j.pharmthera.2020.107517>. Epub 2020 Feb 25. PMID: 32109491.
- [3] B. Blechacz, Cholangiocarcinoma: current knowledge and new developments, Gut Liver 11 (1) (2017 Jan 15) 13–26, <https://doi.org/10.5009/gnl15568>. PMID: 27928095; PMCID: PMC5221857.
- [4] P. Bertuccio, M. Malvezzi, G. Carioli, D. Hashim, P. Boffetta, H.B. El-Serag, C. La Vecchia, E. Negri, Global trends in mortality from intrahepatic and extrahepatic cholangiocarcinoma, J. Hepatol. 71 (1) (2019 Jul) 104–114, <https://doi.org/10.1016/j.jhep.2019.03.013>. Epub 2019 Mar 23. PMID: 30910538.
- [5] B. Sripa, P.J. Brindley, J. Mulvenna, T. Laha, M.J. Smout, E. Mairiang, J. M. Bethony, A. Loukas, The tumorigenic liver fluke *Opisthorchis viverrini*-multiple pathways to cancer, Trends Parasitol. 28 (10) (2012 Oct) 395–407, <https://doi.org/10.1016/j.pt.2012.07.006>. Epub 2012 Sep 1. PMID: 22947297; PMCID: PMC3682777.
- [6] F. Turati, P. Bertuccio, E. Negri, C.L. Vecchia, Epidemiology of cholangiocarcinoma, Hepatoma Res 8 (2022) 19, <https://doi.org/10.20517/2394-5079.2021.130>.
- [7] S. Kamsa-Ard, V. Luvira, K. Suwanrungruang, S. Kamsa-Ard, V. Luvira, C. Santong, T. Srisuk, A. Pugkhem, V. Bhudhisawasdi, C. Pairojkul, Cholangiocarcinoma trends, incidence, and relative survival in Khon Kaen, Thailand from 1989 through 2013: a population-based cancer registry study, J. Epidemiol. 29 (5) (2019 May 5) 197–204, <https://doi.org/10.2188/jea.JE20180007>. Epub 2018 Aug 4. Erratum in: J Epidemiol. 2020;30(2):108–109. PMID: 30078813; PMCID: PMC6445798.
- [8] M.A. Lowery, R. Ptashkin, E. Jordan, M.F. Berger, A. Zehir, M. Capani, N. E. Kemeny, E.M. O'Reilly, I. El-Dika, W.R. Jarnagin, J.J. Harding, M.I. D'Angelica, A. Cerce, J.F. Hechtman, D.B. Solit, N. Schultz, D.M. Hyman, D.S. Klimstra, L. B. Saltz, G.K. Abou-Alfa, Comprehensive molecular profiling of intrahepatic and extrahepatic cholangiocarcinomas: potential targets for intervention, Clin. Cancer Res. 24 (17) (2018 Sep 1) 4154–4161, <https://doi.org/10.1158/1078-0432.CCR-18-0078>. Epub 2018 May 30. PMID: 29848569; PMCID: PMC6462361.
- [9] A.A. Rahnamai-Azar, A. Abbasi, A.W. Acher, S.M. Weber, T.M. Pawlik, Emerging pathways for precision medicine in management of cholangiocarcinoma, Surg Oncol 35 (2020 Dec) 47–55, <https://doi.org/10.1016/j.suronc.2020.08.008>. Epub 2020 Aug 12. PMID: 32827952.
- [10] S. Brivio, M. Cadamuro, M. Strazzabosco, L. Fabris, Tumor reactive stroma in cholangiocarcinoma: the fuel behind cancer aggressiveness, World J. Hepatol. 9 (9) (2017 Mar 28) 455–468, <https://doi.org/10.4245/wjh.v9.i9.455>. PMID: 28396716; PMCID: PMC5368623.
- [11] A.E. Sirica, G.J. Gores, Desmoplastic stroma and cholangiocarcinoma: clinical implications and therapeutic targeting, Hepatology 59 (6) (2014 Jun) 2397–2402, <https://doi.org/10.1002/hep.26762>. Epub 2014 Apr 9. PMID: 24123296; PMCID: PMC3975806.
- [12] M.E. Argenziano, M. Montori, C. Scorzoni, A. Benedetti, M. Marzoni, L. Maroni, The role of tumor microenvironment in cholangiocarcinoma, Hepatoma Res 9 (2023) 9, <https://doi.org/10.20517/2394-5079.2022.98>.
- [13] A. Gentilini, M. Pastore, F. Marra, C. Raggi, The role of stroma in cholangiocarcinoma: the intriguing interplay between fibroblastic component, immune cell subsets and tumor epithelium, Int. J. Mol. Sci. 19 (10) (2018 Sep 22) 2885, <https://doi.org/10.3390/ijms19102885>. PMID: 30249019; PMCID: PMC6213545.
- [14] M. Cadamuro, T. Stecca, S. Brivio, V. Mariotti, R. Fiorotto, C. Spirli, M. Strazzabosco, L. Fabris, The deleterious interplay between tumor epithelia and stroma in cholangiocarcinoma, Biochim. Biophys. Acta, Mol. Basis Dis. 1864 (4 Pt 1) 1–10, <https://doi.org/10.1016/j.bbamol.2023.186401>. Epub 2023 Nov 15. PMID: 37982200; PMCID: PMC9700000.

- B) (2018 Apr) 1435–1443, <https://doi.org/10.1016/j.bbadi.2017.07.028>. Epub 2017 Jul 27. PMID: 28757170; PMCID: PMC6386155.
- [15] A.E. Sirica, The role of cancer-associated myofibroblasts in intrahepatic cholangiocarcinoma, *Nat. Rev. Gastroenterol. Hepatol.* 9 (1) (2011 Nov 29) 44–54, <https://doi.org/10.1038/nrgastro.2011.222>. PMID: 22143274.
- [16] S. Thongchot, C. Vidoni, A. Ferraresi, W. Loilome, N. Khuntikeo, S. Sangkhamanon, A. Titapun, C. Isidoro, N. Namwat, Cancer-associated fibroblast-derived IL-6 determines unfavorable prognosis in cholangiocarcinoma by affecting autophagy-associated chemoresponse, *Cancers* 13 (9) (2021 Apr 28) 2134, <https://doi.org/10.3390/cancers13092134>. PMID: 33925189; PMCID: PMC8124468.
- [17] Y. Kittirat, M. Suksawat, S. Thongchot, S. Padthaisong, J. Phetcharaburanan, A. Wangwiwatsin, P. Klanrit, S. Sangkhamanon, A. Titapun, W. Loilome, H. Saya, N. Namwat, Interleukin-6-derived cancer-associated fibroblasts activate STAT3 pathway contributing to gemcitabine resistance in cholangiocarcinoma, *Front. Pharmacol.* 13 (2022 Aug 26), 897368, <https://doi.org/10.3389/fphar.2022.897368>. PMID: 36091805; PMCID: PMC9459012.
- [18] M. Montori, C. Scorzoni, M.E. Argenziano, D. Baldacci, F. De Blasio, F. Martini, T. Buono, A. Benedetti, M. Marzoni, L. Maroni, Cancer-associated fibroblasts in cholangiocarcinoma: current knowledge and possible implications for therapy, *J. Clin. Med.* 11 (21) (2022 Nov 2) 6498, <https://doi.org/10.3390/jcm11216498>. PMID: 36362726; PMCID: PMC9654416.
- [19] S. Thongchot, A. Ferraresi, C. Vidoni, W. Loilome, P. Yongvanit, N. Namwat, C. Isidoro, Resveratrol interrupts the pro-invasive communication between cancer associated fibroblasts and cholangiocarcinoma cells, *Cancer Lett.* 430 (2018 Aug 28) 160–171, <https://doi.org/10.1016/j.canlet.2018.05.031>. Epub 2018 May 23. Erratum in: *Cancer Lett.* 2018 Oct 10;434:206–207. PMID: 29802929.
- [20] A. Ferraresi, R. Titone, C. Follo, A. Castiglioni, G. Chiorino, D.N. Dhanasekaran, C. Isidoro, The protein restriction mimetic Resveratrol is an autophagy inducer stronger than amino acid starvation in ovarian cancer cells, *Mol. Carcinog.* 56 (12) (2017 Dec) 2681–2691, <https://doi.org/10.1002/mc.22711>. Epub 2017 Sep 7. PMID: 28856729.
- [21] B. Ren, M.X. Khaw, C. Liu, Z. Ma, M.K. Shanmugam, L. Ding, X. Xiang, P.C. Ho, L. Wang, P.S. Ong, B.C. Goh, Resveratrol for cancer therapy: challenges and future perspectives, *Cancer Lett.* 515 (2021 Sep 1) 63–72, <https://doi.org/10.1016/j.canlet.2021.05.001>. Epub 2021 May 28. PMID: 34052324.
- [22] B. Song, W. Wang, X. Tang, R.M.W. Goh, W.L. Thuya, P.C.L. Ho, L. Chen, L. Wang, Inhibitory potential of resveratrol in cancer metastasis: from biology to therapy, *Cancers* 15 (10) (2023 May 14) 2758, <https://doi.org/10.3390/cancers15102758>. PMID: 37345095; PMCID: PMC10216034.
- [23] G. Hather, R. Liu, S. Bandi, J. Mettetal, M. Manfredi, W.C. Shyu, J. Donelan, A. Chakravarti, Growth rate analysis and efficient experimental design for tumor xenograft studies, *Cancer Inf.* 13 (Suppl 4) (2014 Dec 9) 65–72, <https://doi.org/10.4137/CIN.S13974>. PMID: 25574127; PMCID: PMC4264612.
- [24] A. Ferraresi, A. Esposito, C. Girone, L. Vallino, A. Salwa, I. Ghezzi, S. Thongchot, C. Vidoni, D.N. Dhanasekaran, C. Isidoro, Resveratrol contrasts LPA-induced ovarian cancer cell migration and platinum resistance by rescuing hedgehog-mediated autophagy, *Cells* 10 (11) (2021 Nov 17) 3213, <https://doi.org/10.3390/cells10113213>. PMID: 34831435; PMCID: PMC8625920.
- [25] N.F. Trinchieri, C. Follo, G. Nicotra, C. Peracchio, R. Castino, C. Isidoro, Resveratrol-induced apoptosis depends on the lipid kinase activity of Vps34 and on the formation of autophagolysosomes, *Carcinogenesis* 29 (2) (2008 Feb) 381–389, <https://doi.org/10.1093/carcin/bgm271>. Epub 2007 Nov 28. PMID: 18048384.
- [26] M. Savio, A. Ferraresi, C. Corpina, S. Vandenberghe, C. Scarlata, V. Sottile, L. Morini, B. Garavaglia, C. Isidoro, L.A. Stivala, Resveratrol and its analogue 4,4'-Dihydroxy-trans-stilbene inhibit lewis lung carcinoma growth in vivo through apoptosis, autophagy and modulation of the tumour microenvironment in a murine model, *Biomedicines* 10 (8) (2022 Jul 25) 1784, <https://doi.org/10.3390/biomedicines10081784>. PMID: 35892684; PMCID: PMC9332680.
- [27] L. Tan, W. Wang, G. He, R.D. Kuick, G. Gossner, A.S. Kueck, H. Wahl, A.W. Opipari, J.R. Liu, Resveratrol inhibits ovarian tumor growth in an in vivo mouse model, *Cancer* 122 (5) (2016 Mar 1) 722–729, <https://doi.org/10.1002/cncr.29793>. Epub 2015 Nov 30. PMID: 26619367.
- [28] D.J. Klionsky, A.K. Abdel-Aziz, S. Abdelfatah, M. Abdellatif, A. Abdoli, S. Abel, et al., Guidelines for the use and interpretation of assays for monitoring autophagy (4th edition) 1, *Autophagy* 17 (1) (2021 Jan) 1–382, <https://doi.org/10.1080/15548627.2020.1797280>. Epub 2021 Feb 8. PMID: 33634751; PMCID: PMC7996087.
- [29] H. Folkerts, S. Hilgendorf, E. Vellenga, E. Bremer, V.R. Wiersma, The multifaceted role of autophagy in cancer and the microenvironment, *Med. Res. Rev.* 39 (2) (2019 Mar) 517–560, <https://doi.org/10.1002/med.21531>. Epub 2018 Oct 9. PMID: 30302772; PMCID: PMC6585651.
- [30] T. Monkonen, J. Debnath, Inflammatory signaling cascades and autophagy in cancer, *Autophagy* 14 (2) (2018) 190–198, <https://doi.org/10.1080/15548627.2017.1345412>. Epub 2017 Sep 18. PMID: 28813180; PMCID: PMC5902219.
- [31] C. Thuwajit, A. Ferraresi, R. Titone, P. Thuwajit, C. Isidoro, The metabolic cross-talk between epithelial cancer cells and stromal fibroblasts in ovarian cancer progression: autophagy plays a role, *Med. Res. Rev.* 38 (4) (2018 Jul) 1235–1254, <https://doi.org/10.1002/med.21473>. Epub 2017 Sep 19. PMID: 28926101; PMCID: PMC6032948.
- [32] A. Ferraresi, C. Girone, A. Esposito, C. Vidoni, L. Vallino, E. Secomandi, D. N. Dhanasekaran, C. Isidoro, How autophagy shapes the tumor microenvironment in ovarian cancer, *Front. Oncol.* 10 (2020 Dec 7), 599915, <https://doi.org/10.3389/fonc.2020.599915>. PMID: 33364196; PMCID: PMC7753622.
- [33] A. Ferraresi, S. Phadnang, F. Morani, A. Galetto, O. Alabiso, G. Chiorino, C. Isidoro, Resveratrol inhibits IL-6-induced ovarian cancer cell migration through epigenetic up-regulation of autophagy, *Mol. Carcinog.* 56 (3) (2017 Mar) 1164–1181, <https://doi.org/10.1002/mc.22582>. Epub 2016 Nov 3. PMID: 27787915.
- [34] Y. Chen, X. Zhang, H. Yang, T. Liang, X. Bai, The "Self-eating" of cancer-associated fibroblast: a potential target for cancer, *Biomed. Pharmacother.* 163 (2023 Jul), 114762, <https://doi.org/10.1016/j.biopha.2023.114762>. Epub 2023 Apr 24. PMID: 37100015.
- [35] S. Garvin, K. Ollinger, C. Dabrosin, Resveratrol induces apoptosis and inhibits angiogenesis in human breast cancer xenografts in vivo, *Cancer Lett.* 231 (1) (2006 Jan 8) 113–122, <https://doi.org/10.1016/j.canlet.2005.01.031>. PMID: 16356836.
- [36] T. Sudha, A.H. El-Far, D.S. Mousa, S.A. Mousa, Resveratrol and its nanoformulation attenuate growth and the angiogenesis of xenograft and orthotopic colon cancer models, *Molecules* 25 (6) (2020 Mar 20) 1412, <https://doi.org/10.3390/molecules25061412>. PMID: 32244860; PMCID: PMC7144556.
- [37] C. Vidoni, A. Ferraresi, L. Vallino, A. Salwa, J.H. Ha, C. Seca, B. Garavaglia, D. N. Dhanasekaran, C. Isidoro, Glycolysis inhibition of autophagy drives malignancy in ovarian cancer: exacerbation by IL-6 and attenuation by resveratrol, *Int. J. Mol. Sci.* 24 (2) (2023 Jan 15) 1723, <https://doi.org/10.3390/ijms24021723>. PMID: 36675246; PMCID: PMC9866176.
- [38] D. Wang, H. Guo, H. Yang, D. Wang, P. Gao, W. Wei, Pterostilbene, an active constituent of blueberries, suppresses proliferation potential of human cholangiocarcinoma via enhancing the autophagic flux, *Front. Pharmacol.* 10 (2019 Oct 22) 1238, <https://doi.org/10.3389/fphar.2019.01238>. PMID: 3195612; PMCID: PMC6817474.
- [39] J. Suh, D.H. Kim, Y.J. Suh, Resveratrol suppresses migration, invasion and stemness of human breast cancer cells by interfering with tumor-stromal cross-talk, *Arch. Biochem. Biophys.* 643 (2018 Apr 2) 62–71, <https://doi.org/10.1016/j.abb.2018.02.011>. PMID: PMC29477771.
- [40] M. Sasaki, T. Nitta, Y. Sato, Y. Nakamura, Autophagy may occur at an early stage of cholangiocarcinogenesis via biliary intraepithelial neoplasia, *Hum. Pathol.* 46 (2) (2015 Feb) 202–209, <https://doi.org/10.1016/j.humpath.2014.09.016>. Epub 2014 Oct 23. PMID: 25466963.
- [41] T.T. Wang, Q.H. Cao, M.Y. Chen, Q. Xia, X.J. Fan, X.K. Ma, Q. Lin, C.C. Jia, M. Dong, D.Y. Ruan, Z.X. Lin, J.Y. Wen, L. Wei, X. Li, Z.H. Chen, L. Wang, X.Y. Wu, X.B. Wan, Beclin 1 deficiency correlated with lymph node metastasis, predicts a distinct outcome in intrahepatic and extrahepatic cholangiocarcinoma, *PLoS One* 8 (11) (2013 Nov 26), e80317, <https://doi.org/10.1371/journal.pone.0080317>. PMID: 24303007; PMCID: PMC3841169.
- [42] D.S. Perng, C.M. Hung, H.Y. Lin, P. Morgan, Y.C. Hsu, T.C. Wu, P.M. Hsieh, J. H. Yeh, P. Hsiao, C.Y. Lee, Y.C. Li, Y.C. Wang, Y.S. Chen, C.W. Lin, Role of autophagy-related protein in the prognosis of combined hepatocellular carcinoma and cholangiocarcinoma after surgical resection, *BMC Cancer* 21 (1) (2021 Jul 17) 828, <https://doi.org/10.1186/s12885-021-08553-6>. PMID: 34273969; PMCID: PMC8286562.
- [43] G. Lendvai, T. Szekerczés, I. Illyés, M. Csengeri, K. Schlachter, E. Szabó, G. Lotz, A. Kiss, B. Korka, Z. Schaff, Autophagy activity in cholangiocarcinoma is associated with anatomical localization of the tumor, *PLoS One* 16 (6) (2021 Jun 15), e0253065, <https://doi.org/10.1371/journal.pone.0253065>. PMID: 34129628; PMCID: PMC8205141.
- [44] A. Esposito, A. Ferraresi, A. Salwa, C. Vidoni, D.N. Dhanasekaran, C. Isidoro, Resveratrol contrasts IL-6 pro-growth effects and promotes autophagy-mediated cancer cell dormancy in 3D ovarian cancer: role of miR-1305 and of its target ARH-I, *Cancer* 14 (9) (2022 Apr 25) 2142, <https://doi.org/10.3390/cancers14092142>. PMID: 35565270; PMCID: PMC9101105.
- [45] M.S. Sosa, P. Bragado, J. Debnath, J.A. Aguirre-Ghiso, Regulation of tumor cell dormancy by tissue microenvironments and autophagy, *Adv. Exp. Med. Biol.* 734 (2013) 73–89, https://doi.org/10.1007/978-1-4614-1445-2_5. PMID: 23143976; PMCID: PMC3651695.
- [46] C. Jakobović Brala, A. Karković Marković, A. Kugić, J. Torić, M. Barbarić, Combination chemotherapy with selected polyphenols in preclinical and clinical studies—an update overview, *Molecules* 28 (9) (2023 Apr 26) 3746, <https://doi.org/10.3390/molecules28093746>. PMID: 37175156; PMCID: PMC10180288.
- [47] J. Fang, C. Cai, Q. Wang, P. Lin, Z. Zhao, F. Cheng, Systems pharmacology-based discovery of natural products for precision oncology through targeting cancer mutated genes, *CPT Pharmacometrics Syst. Pharmacol.* 6 (3) (2017 Mar) 177–187, <https://doi.org/10.1002/psp.4.12172>. Epub 2017 Mar 14. PMID: 28294568; PMCID: PMC5356618.